Measurements of Dijet Cross-Section at Low Q^2 and the Extraction of an Effective Parton Density for the Virtual Photon

N.Z. Gogitidze[a*]

[a]DESY, Notkestrasse 85, D-22603 Hamburg, Germany
and P.N. Lebedev Physical Institute RAS, 117924 Moscow, Russia

The triple-differential dijet cross-section, $\mathrm{d}^3\sigma_{ep}/\mathrm{d}Q^2\mathrm{d}\overline{E_t}^2\mathrm{d}x_\gamma^{jets}$, is measured with the H1 detector at HERA as a function of the photon virtuality Q^2, the fraction of the photon's momentum carried by the parton entering the hard scattering, x_γ^{jets}, and the square of the mean transverse energy, $\overline{E_t}^2$, of the two highest E_t jets. Jets are found using a longitudinal boost-invariant k_T clustering algorithm in the $\gamma^* p$ center of mass frame. The measurements cover the ranges $1.6 < Q^2 < 80$ GeV^2 in virtuality and $0.1 < y < 0.7$ in inelasticity y. The results are well described by leading order QCD models which include the effects of a resolved component to the virtual photon. Models which treat the photon as point-like fail to describe the data. An effective leading order parton density for the virtual photon is extracted as a function of the photon virtuality, the probing scale and the parton momentum fraction. The x_γ and probing scale dependences of the parton density show characteristic features of photon structure, and a suppression of this structure with increasing Q^2 is seen.

1. INTRODUCTION

At e^+e^- and ep colliders, photons are emitted by the leptons in a wide range of photon virtuality Q^2. This allows to be studied the partonic structure of almost real photons, as well as of virtual photons. Measurements to obtain information on the partonic structure of the photon have been carried out at several e^+e^- colliders (PETRA, PEP, TRISTAN, LEP) [1] and in recent years also at the HERA ep collider [2]. A compilation of these measurements is shown in Figure 1 as a function of the resolution scale Q^2, at average $x \sim 0.5$; x is the fraction of the photon momentum carried by the parton. [3]. The data are compatible with an increasing parton density in the photon as Q^2 increases. This Q^2 dependence is expected in perturbative QCD (pQCD): the splitting of the photon into a $q\bar{q}$ pair gives in leading order rise to the probability $f_{q/\gamma}$ of finding a quark in the photon, and $f_{q/\gamma} \sim \ln(Q^2/\Lambda^2_{QCD})$. In Figure 1 is also shown an effective parton distribution $x\tilde{f}_\gamma$ of the photon, extracted from dijet measurements in γp collisions by the H1 collaboration at HERA. The relevant resolution scale is here the transverse momentum squared, P_t^2, of the scattered partons. The results of the dijet measurements are in good agreement with the F_2^γ data. The jet data probe the partons of the photon at large resolution scales and compete well in precision with the F_2^γ measurements.

The QCD picture of the photon structure can be further tested by increasing the mass squared P^2 of the target photon. The only such measurement until recently was made by the PLUTO experiment at PETRA in the early 1980s [4][2]. The results demonstrate that, as the mass of the target photon increases its hadronic structure diminishes. This is predicted in perturbative QCD and the interesting question then arises: what happens at still larger target photon masses? The answer to this question can be obtained at the HERA ep collider, where the mass of the target photon can be substantially increased.

The cross-section for high transverse momentum (P_t) jet production in ep collisions is dominated by processes in which the exchanged pho-

*On behalf of the H1 Collaboration

[2]New results from LEP have been presented at this conference, see further reports in these proceedings.

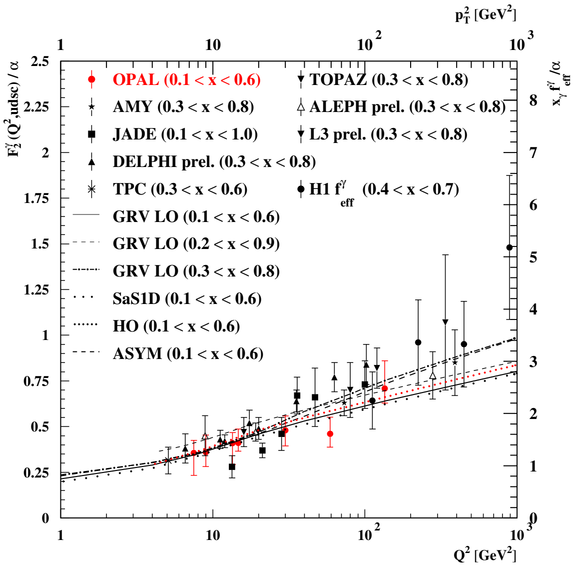

Figure 1. Measurements from e^+ e^- data of the photon structure function F_2^γ as a function of the virtuality Q^2 of the probing photon for the fraction of the photon momenta $x \sim 0.5$ are shown in comparison with an effective parton distribution extracted from photoproduction of dijets in ep collisions at HERA (H1 data). The curves represent different parametrizations of the parton distributions of the photon.

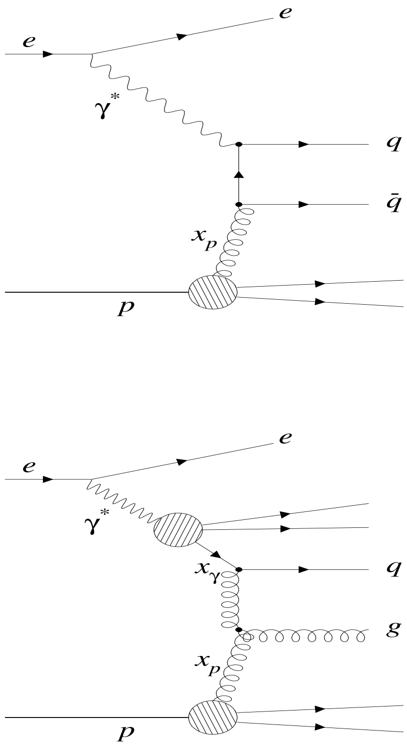

Figure 2. Leading order Feynman diagrams of dijet production in $\gamma^* p$ collisions. The top diagram shows the direct process, while the bottom diagram shows the resolved process.

ton is quasi-real (photoproduction processes). Two types of interaction can be distinguished in leading order: direct processes, where the photon couples as a point-like object to a parton from the proton, and resolved processes, where the photon develops a partonic structure prior to the collision (Figure 2). In the latter case a parton out of the photon, carrying only a fraction x_γ of the photon momentum, enters the hard scattering process leading to the production of jets. The photoproduction jet cross-section is sensitive to the density of partons in the photon at the scale P_t^2 of the jets.

The diagrams in Figure 2 are equally applicable to processes where the exchanged photon is virtual. In such deep-inelastic scattering interactions, the production of high E_t jets is usually dominated by direct processes. However, as long as the photon is probed with sufficiently high resolution ($P_t^2 >> Q^2$) the cross-section will still be sensitive to the photon parton density. Perturbative QCD predicts that the parton density of the photon at fixed P_t^2 should be suppressed with increasing Q^2 and that the structure should simplify to direct coupling to a $q\bar{q}$ pair.

2. THE TRIPLE DIFFERENTIAL DIJET CROSS-SECTION

The data presented here [5] were taken during 1996 when HERA was colliding 27.5 GeV positrons with 820 GeV protons, and correspond to an integrated luminosity of $\sim 6\ pb^{-1}$.

In the triple differential dijet cross-section, $d^3\sigma/dQ^2 d\overline{E}_t^2 dx_\gamma^{jets}$, $\overline{E}_t^2$ is the mean of the transverse energies of the two highest E$_t$ jets measured in the $\gamma^* p$ mass frame and x_γ^{jets} is the value of x_γ reconstructed from the jets:

$$x_\gamma^{jets} = \frac{\sum_{jets}(E^{jet} - p_z^{jet})}{\sum_h (E^h - p_z^h)}$$

where the sum in the denominator is over all final state particles except the scattered positron. The kinematic range $1.6 < Q^2 < 80$ GeV^2 in virtuality and $0.1 < y < 0.7$ in inelasticity is covered by the data. Jets were reconstructed in the hadronic center of mass system using the inclusive k_T clustering algorithm [6]. Events were requested to contain at least two jets, and were accepted if the two highest E$_t$ jets satisfied the cuts:

- $|\eta_1^{jet} - \eta_2^{jet}| < 1.0$
- -3.0 $< \overline{\eta} <$ -0.5
- $\overline{E}_t^2 < 30$ GeV^2
- $\frac{|(E_t^{jet1} - E_t^{jet2})|}{(E_t^{jet1} + E_t^{jet2})} < 0.25$

These cuts ensure that the jets are confined to a region in the detector, where they can be well measured. After application of these selection criteria a sample of approximately 12,000 dijet events was obtained.

Figure 3 shows the dijet cross-section as a function of x_γ^{jets} for different ranges of $\overline{E}_t^2$ and Q^2. In all bins of Q^2 and $\overline{E}_t^2$ the x_γ^{jets} distribution peaks towards $x_\gamma^{jets} = 1$, where the direct photon contribution is concentrated. There is a strong decrease in the cross-section with increasing $\overline{E}_t^2$. The relative contribution from resolved photons, in the region $x_\gamma^{jets} \leq 0.75$, diminishes as Q^2 increases at fixed $\overline{E}_t^2$. Note that the reduction in the cross-section in the lowest x_γ^{jets} bin is a consequence of the cuts in $\overline{\eta}$ and $\overline{E}_t^2$. The absence of a data point indicates that no measurement was made in that bin due to insufficient statistics.

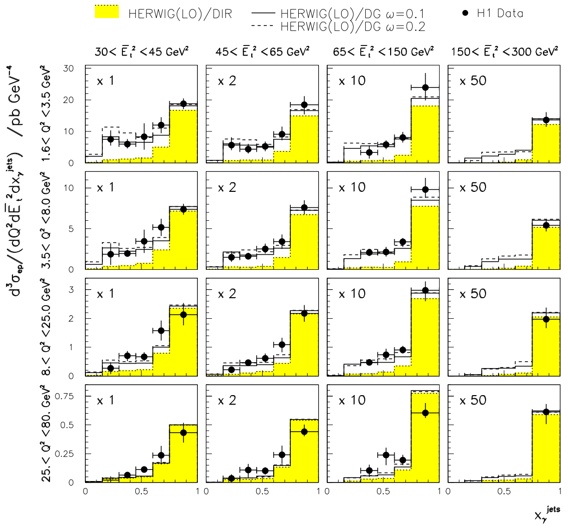

Figure 3. The differential dijet cross-section $d^3\sigma/dQ^2 d\overline{E_t^2} dx_\gamma^{jets}$ as a function of x_γ^{jets} for different regions of $\overline{E_t^2}$ and Q^2. The scale factors applied to the cross-sections are indicated. Predictions from a LO model, which includes a resolved component in the virtual photon, are also shown (dotted and dashed histograms) together with the direct photon component of this model (shaded histogram).

The data are compared with predictions of several models with LO matrix elements and parton densities [7,8]. The HERWIG(LO)/DG simulation is shown for two choices of the Q^2 suppression factor, ω. The model prediction for the direct only contribution is also shown. With $\omega = 0.1$ GeV, the HERWIG(LO)/DG model gives a reasonable description of the cross-section throughout the Q^2 - $\overline{E}_t^2$ range. Increasing ω to 0.2 GeV leads to an overestimation in the low Q^2, low $\overline{E}_t^2$ regions. However, the value of ω which best describes the data, depends on the frequency of soft underlying events. The RAPGAP(LO)/DG model prediction (not shown in this figure), which contains no soft underlying event, requires $\omega \sim 0.2$ GeV in order to describe the data. As Q^2 increases, both HERWIG models tend to underestimate the cross-section for intermediate x_γ^{jets} values and overestimate it at high x_γ^{jets}. The direct only contribution is able to describe the data in the highest x_γ^{jets} bin, but underestimates the data for $x_\gamma^{jets} \leq 0.75$, except possibly in the highest Q^2 range.

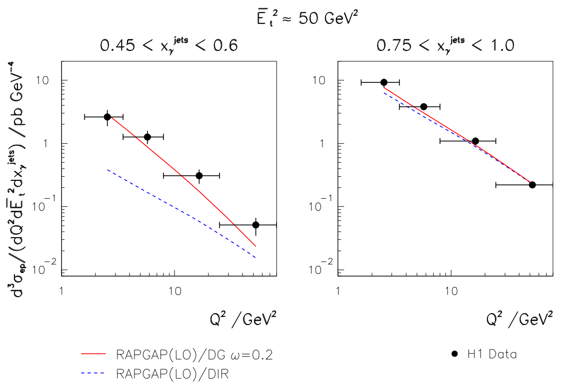

Figure 4. The differential dijet cross-section as a function of Q^2 for two different x_γ^{jets} regions and $\overline{E_t^2} = 50$ GeV^2. Also shown are the predictions from the RAPGAP(LO)/DG model (full curve) and the direct photon processes in this model (dashed curve).

The Q^2 dependence of the cross-section is shown in Figure 4 for the fixed value of $\overline{E}_t^2 = 50$ GeV^2 and two bins of x_γ^{jets}. There is a steep decrease in the cross-section with Q^2, but the rate of decrease becomes smaller as x_γ^{jets} increases. This behaviour is well described by the RAPGAP(LO)/DG model. The expectation from the direct-only component of RAPGAP predicts a rate of suppression of the cross-section, which is lower than seen in the data, except for $x_\gamma^{jets} > 0.75$ where the point-like processes dominate the cross-section. This is indicative of additional suppression arising from the photon parton densities.

From the above comparisons we can conclude that the observed dependence of the triple differential dijet cross-section is consistent with that predicted for a resolved virtual photon with parton density functions evolving with Q^2 according to QCD motivated models.

3. EFFECTIVE PARTON DENSITY OF THE VIRTUAL PHOTON

To extract the effective parton density of the virtual photon from the dijet cross-sections, the Single Effective Subprocess Approximation has been used [9]. It exploits the fact that the dominant contributions to the cross-section comes from parton-parton scattering matrix elements that have similar shapes and so differ mainly by their associated color factors. Thus the sum over processes in the cross-section for the production of dijets by resolved virtual photons can be replaced by a single effective sub-process cross-section and effective parton densities. The effective parton density for the photon is defined as:

$$\tilde{f}_\gamma(x_\gamma, P_t^2, Q^2) = \sum_{nf}(f_{q/\gamma}(x_\gamma, P_t^2, Q^2) +$$

$$+ f_{\bar{q}/\gamma}(x_\gamma, P_t^2, Q^2)) + \frac{9}{4} f_{g/\gamma}(x_\gamma, P_t^2, Q^2)$$

The measured parton density is polarization averaged:

$$f_{i/\gamma}(x_\gamma, P_t^2, Q^2) \equiv$$

$$\equiv f_{i/\gamma}^T(x_\gamma, P_t^2, Q^2) + \overline{\epsilon} f_{i/\gamma}^L(x_\gamma, P_t^2, Q^2)$$

$\overline{\epsilon} \sim 1$ is the ratio of longitudinal to transverse photon fluxes, averaged over the y - range of the data. $f_{i/\gamma}^L$ is expected to be small over most of the kinematic range considered here [12–14].

In Figure 5 the extracted effective parton density is shown as a function of the probing scale P_t^2 for different values of Q^2 and x_γ. Only points where $\langle P_t^2 \rangle > \langle Q^2 \rangle$ are shown. The scale dependence contrasts with the falling behaviour expected for hadronic parton densities and, within the large systematic errors, is consistent with the logarithmic scale dependence predicted by perturbative QCD for the point-like coupling of

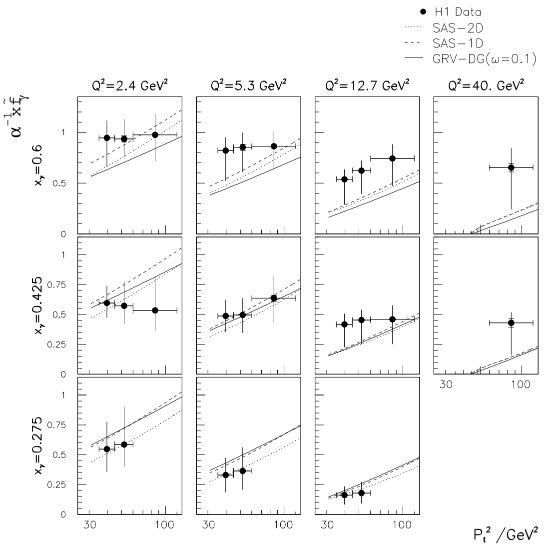

Figure 5. The leading order effective parton density of the photon $x_\gamma \tilde{f}_\gamma$, as a function of P_t^2 for different values of Q^2 and x_γ.

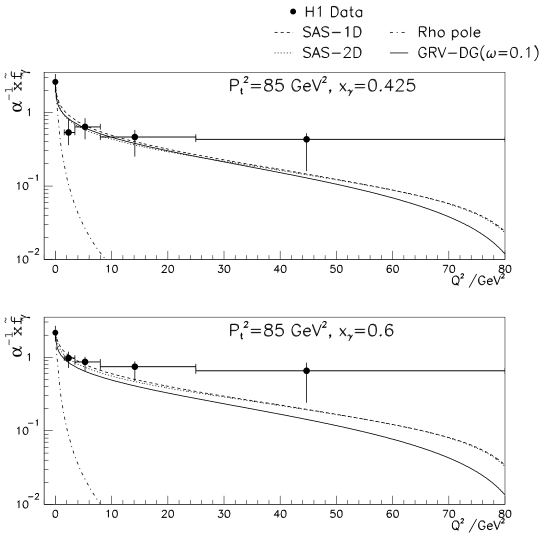

Figure 6. The leading order effective parton density of the photon $x_\gamma \tilde{f}_\gamma$ as a function of Q^2, for $\mathrm{P}_t^2 = 85\ \mathrm{GeV}^2$ and two values of x_γ.

the photon to a $q\bar{q}$ pair. The data are compared with several QCD inspired parametrisations [8,10] which are all in reasonable agreement with the measured values.

Figure 6 shows the Q^2 evolution of the effective parton density for $\mathrm{P}_t^2 = 85\ \mathrm{GeV}^2$ and two ranges of x_γ: $0.35 < x_\gamma < 0.5$ and $0.5 < x_\gamma < 0.7$. Superimposed on the same plots are photoproduction measurements at $\mathrm{P}_t^2 = 112\ \mathrm{GeV}^2$ and x_γ values of 0.3 and 0.55 [11], which have been extrapolated to the P_t^2 and x_γ values in the figure. The extrapolation was based on the GRV-LO parton densities which give a good description of the photoproduction data. A clear suppression with Q^2 can be seen. The QCD inspired parametrisations which predict a logarithmic suppression with Q^2 are in reasonable agreement with the data. At high Q^2 the parton densities are suppressed more slowly than the models predict. Also shown is a simple ρ - pole suppression factor characteristic of a pure VMD model:

$$f_{i/\gamma}(x_\gamma, P_t^2, Q^2) \sim f_{i/\gamma}(x_\gamma, P_t^2, 0) \left(\frac{m_\rho^2}{m_\rho^2 + Q^2} \right)^2$$

The latter clearly underestimates the data.

4. CONCLUSIONS

Dijet production data in the Q^2 range $0 \leq Q^2 \leq 80\ \mathrm{GeV}^2$ show clear evidence for the virtual photon structure.

The triple differential cross-section $d^3\sigma_{ep}/dQ^2 d\overline{E}_t^2 dx_\gamma^{jets}$ is measured in dijet events for $1.6 < Q^2 < 80\ \mathrm{GeV}^2$ and $0.1 < y < 0.7$. The cross-section shows the x_γ^{jets}, $\overline{E}_t^2$, Q^2 behaviour expected for processes in which a virtual photon, carrying a hadronic structure evolving according to perturbative QCD. As $Q^2 \to \overline{E}_t^2$, the photon structure reduces to a simple direct coupling to $q\bar{q}$ pairs and the dijet cross-section is well described without invoking photon structure.

For the first time an effective, leading order parton density of the virtual photon has been extracted in the Single Effective Subprocess approximation and its dependence on x_γ, target virtuality Q^2 and probing scale P_t^2 has been measured. The photon parton density shows the logarithmic scaling characteristic of photon structure and is seen to be suppressed with increasing Q^2 as predicted by perturbative QCD.

ACKNOWLEDGEMENTS

It is a pleasure for me to thank all my colleagues in H1 for useful discussions and help in preparing the report. I would also like to thank the organizers for hospitality and for creating a pleasant and inspiring conference atmosphere.

REFERENCES

1. PLUTO Collab., Ch. Berger et al., Phys. Lett. B107 (1981) 168;
   JADE Collab., W.Bartel et al., Z. Phys. C24 (1984) 231;
   TPC/2γ Collab., H. Aihara et al., Phys. Rev. Lett. 58 (1987) 97;
   AMY Collab., T. Sasaki et al., Phys. Lett. B252 (1990) 491;
   OPAL Collab., R. Akers et al., Z. Phys. C61 (1994) 199;
   TOPAZ Collab., H. Hayashii et al., Phys. Lett. B314 (1993);
   ALEPH Collab., D. Buskulic et al., Phys. Lett. B313 (1993) 509;
   DELPHI Collab., P. Abreu et al., Phys. Lett. B342 (1995) 402
2. ZEUS Collab., M. Derrick et al., Phys. lett. B322 (1994) 287;
   H1 Collab., T. Ahmed et al., Nucl. Phys. B445 (1995) 195;
   ZEUS Collab., M. Derrick et al., Phys. lett. B384 (1996) 401;
   ZEUS Collab., J. Breitweg et al., Eur. phys. J. C1 (1998) 109;
   H1 Collab., C. Adloff et al., Eur. phys. J. C1 (1998) 97;
   H1 Collab., S. Aid et al., Z. Phys. C70 (1996) 17
3. M. Erdmann, "Diffraction and Low-Q^2 Physics Including Two-Photon Physics", DESY-98-209
4. PLUTO Collaboration, Ch. Berger et al., Phys. Lett. B142 (1984) 119
5. H1 Collaboration, "Measurement of Dijet Cross-Sections at Low Q^2 and the Extraction of an Effective Parton Density of the Virtual Photon", DESY-98-205, to be published in Eur. Phys. J.C
6. S.D. Ellis and D.E. Soper, Phys. Rev. D48 (1993) 3160
   S. Catani et al., Nucl. Phys. B406 (1993) 187
7. M. Drees and R. Godbole, Phys. Rev. D50 (1994) 3124
8. G. Marchesini et al., Comp. Phys. Comm. 67 (1992) 465
9. B.V. Combridge and C.J.Maxwell, Nucl. Phys. B239 (1984) 429
10. T. Sjöstrand and G.A. Schuler, Phys. Lett. B376 (1996) 193
11. H1 Collaboration, C.Adloff et al., Eur. Phys. J. C1 (1998) 97
12. M.Glück, E.Reya and M. Stratmann, Phys. Rev. D54 (1996) 5515
13. F. Borzumati and G. Schuler, Z. Phys. C58 (1993) 139
14. S. Frixione et al., Phys. Lett. B319 (1993) 339